Top quark properties measurements at the LHC

Mark Owen
On behalf of the ATLAS and CMS Collaborations
School of Physics and Astronomy, University of Glasgow, Glasgow, G12 8QQ, UK

Highlights of measurements of the properties of the top quark at the LHC are presented. The measurements probe a range of the properties of the top quark, including the structure of the Wtb vertex, the top-Z coupling and the top-quark mass. The results are compared to Standard Model predictions and in some cases limits on physics beyond the Standard Model are also extracted in the context of effective field theory models. The measurements use data collected by the ATLAS and CMS experiments during pp collisions at a centre-of-mass energy of 8 or 13 TeV.

1 Introduction

The top quark is the heaviest fundamental particle discovered to date and it decays before it has a chance to hadronise. These characteristics not only allow for precision tests of the Standard Model (SM), but also open a potential window to physics beyond the SM. A selection of recent measurements from the ATLAS [1] and CMS [2] collaborations are discussed below[a]. The measurements use both top-quark pair and single-top quark production modes. For the analyses using $t\bar{t}$ production, two decay modes with low background rates are utilised: the lepton-plus-jets decay mode, where one W boson decays leptonically and the other decays into a pair of quarks and the dilepton decay mode, where both W bosons decays leptonically.

2 The Wtb vertex

In the SM the top quark is predicted to decay almost exclusively into a W boson and b-quark. The decay time of the top quark is shorter than the characteristic time for hadronisation and this means the top quark provides a unique window to observe the properties of a bare quark. The decay products of the top quark can therefore be used to probe the nature of the Wtb vertex.

[a]For a full list of top properties measurements, please see the public websites of the collaborations: http://cms-results.web.cern.ch/cms-results/public-results/publications/TOP/index.html, http://cms-results.web.cern.ch/cms-results/public-results/preliminary-results/TOP/index.html and https://twiki.cern.ch/twiki/bin/view/AtlasPublic/TopPublicResults.

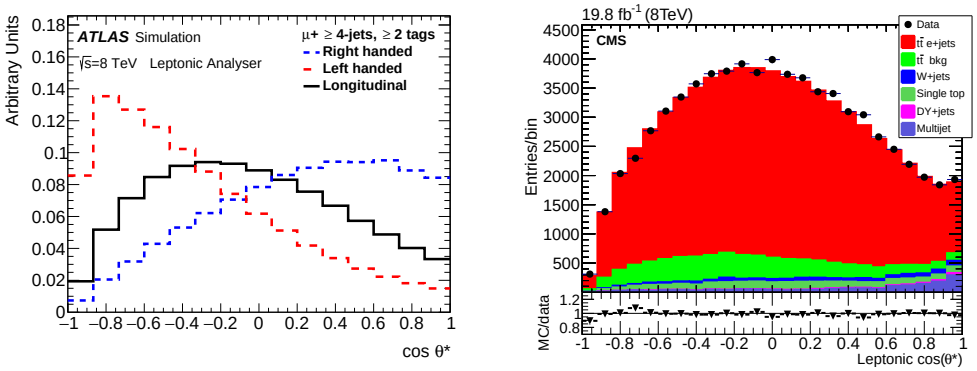

(a) (b)

Figure 1 – Distribution of the cosine of the helicity angle (θ^*) between the charged lepton and the direction of the top quark in the W boson rest frame. (a) Expected distributions for the left-handed, right-handed and longitudinal polarisation states in the ATLAS W polarisation measurement. (b) The CMS data are compared to the SM expectation.

2.1 W boson polarisation

The W bosons produced in top decays can be either left-handed, right-handed or longitudinally polarised. The corresponding fractions (F_{L}, F_{R} and F_0) are well predicted in the SM, however the presence of new physics in the Wtb vertex could result in fractions different to the SM predictions. Experimentally, these fractions can be accessed by measuring the helicity angle θ^* between the charged lepton or down-type quark and the direction of the top quark in the rest frame of the W boson. The distribution for the cosine of the helicity angle depends on the polarisation fractions according to:

$$\frac{1}{\Gamma}\frac{d\Gamma}{d\cos\theta^*} = \frac{3}{8}(1-\cos\theta^*)^2 F_{\mathrm{L}} + \frac{3}{4}(\sin^2\theta^*)F_0 + \frac{3}{8}(1+\cos\theta^*)^2 F_{\mathrm{R}}. \quad (1)$$

The ATLAS and CMS collaborations have both published recent measurements of the W boson polarisation fractions using the 8 TeV LHC data[3,4]. Both experiments select events with one high transverse momentum (p_T) electron or muon and at least four high p_T jets. Kinematic fit techniques are then used to fully reconstruct the $t\bar{t}$ system and the angle θ^* between the charged lepton and the direction of the top quark is then reconstructed in the rest frame of the W boson. The data are fitted to the reconstructed $\cos\theta^*$ distributions in order to extract the measured polarisation fractions. Figure 1 shows the templates in the ATLAS analysis for the left-handed, right-handed and longitudinal polarisation states. There is clear discriminating power between the different polarisation states. The $\cos\theta^*$ distribution measured by CMS is shown in Figure 1 and the data are seen to be in good agreement with the SM predictions. The largest uncertainties in the measurements arise from the Monte Carlo (MC) modelling of top quark events and the jet energy scale (JES). The results are compared to previous LHC results and the SM prediction in Figure 2, where good agreement between the SM and the measurements can be seen.

2.2 Top quark polarisation

Electroweak single-top quark production at the LHC is dominated by t-channel exchange and the top quarks produced are predicted to be highly polarised, in particular along the direction of the spectator-quark momentum [5,6]. The polarisation (P) is related to the angle between a top-quark decay product and the top-quark spin axis (θ_l) according to:

$$\frac{1}{\Gamma}\frac{d\Gamma}{d\cos\theta_l} = \frac{1}{2}(1+\alpha P\cos\theta_l), \quad (2)$$

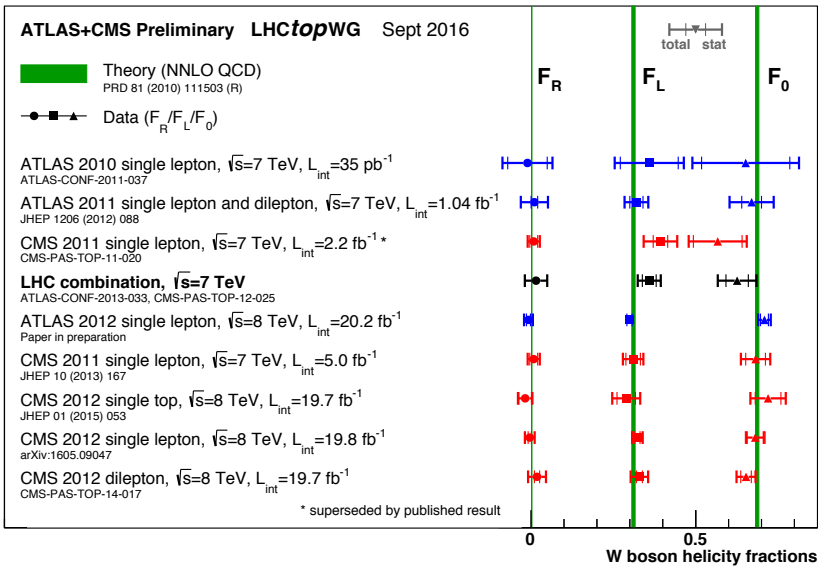

Figure 2 – Summary of LHC measurements of the W boson polarisation fractions.

where α is the spin analysing power of the decay product, which for charged leptons is $\alpha(\ell^{\pm}) = \pm 0.998$ [7].

ATLAS has recently measured [8] a set of angular asymmetries that are sensitive to the top-quark polarisation and six independent W boson spin observables [9]. The measurements use events with one high p_T electron or muon and exactly two jets (one of which must be identified as originating from a b-quark). Selection requirements are imposed to reject the background from W+jets and $t\bar{t}$ events. The measured angular forward-backward asymmetries

$$A_{\mathrm{FB}} = \frac{N(\cos\theta > 0) - N(\cos\theta < 0)}{N(\cos\theta > 0) + N(\cos\theta < 0)} \tag{3}$$

for two angles θ_l and θ_l^N are related to the top polarisation (P) and the W boson spin observable $\langle S_2 \rangle$ according to: $P = 2\frac{A_{\mathrm{FB}}^{\ell}}{\alpha}$ and $\langle S_2 \rangle = -\frac{4}{3}A_{\mathrm{FB}}^{N}$. The values of the observables extracted from the asymmetries are $P = 0.97 \pm 0.12$ and $\langle S_2 \rangle = 0.06 \pm 0.05$. Good agreement is seen between the data and the SM predictions. The CMS experiment has previously measured the polarisation in single top events, finding $P = 0.52 \pm 0.22$ [10]. The measurement agrees within two standard deviations with the SM prediction of 0.9.

2.3 Constraints on the Wtb vertex

If the energy scale of new physics is not directly accessible in top quark production at the LHC, then the impacts of new physics can be parameterised in the effective operator formalism and the most general Wtb Langrangian can be written as:

$$\mathcal{L}_{Wtb} = -\frac{g}{\sqrt{2}}\,\bar{b}\gamma^{\mu}\left(V_{\mathrm{L}}P_{\mathrm{L}} + V_{\mathrm{R}}P_{\mathrm{R}}\right)tW_{\mu}^{-} - \frac{g}{\sqrt{2}}\,\bar{b}\,\frac{i\sigma^{\mu\nu}q_{\nu}}{m_W}\left(g_{\mathrm{L}}P_{\mathrm{L}} + g_{\mathrm{R}}P_{\mathrm{R}}\right)tW_{\mu}^{-} + \mathrm{h.c.} \tag{4}$$

The terms $V_{\mathrm{L,R}}$ and $g_{\mathrm{L,R}}$ are the left- and right-handed vector and tensor couplings, respectively.[b] In the SM at tree-level, V_{L} is the CKM matrix element V_{tb} and the anomalous couplings g_{L}, V_{R} and g_{R} are all zero. The W boson and top-quark polarisation measurements discussed in the previous sections have been used to place limits on the anomalous couplings.

[b] In Equation 4, g is the weak coupling constant, m_W and q_ν are the mass and the four-momentum of the W boson, respectively, $P_{\mathrm{L,R}} \equiv (1 \mp \gamma^5)/2$ are the left- and right-handed projection operators, and $\sigma^{\mu\nu} = [\gamma^{\mu}, \gamma^{\nu}]/2$.

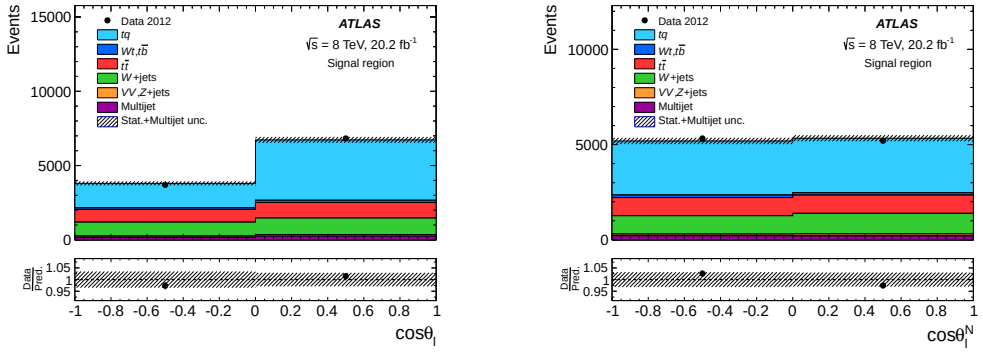

(a) (b)

Figure 3 – Distributions of the cosine of the angles (a) θ_l, which is sensitive to the top-quark polarisation and (b) θ_l^N, which is sensitive to the spin observable $\langle S_2 \rangle$. The data (black points) are compared to the expectation of SM single-top production (light blue) and the background processes (other colours).

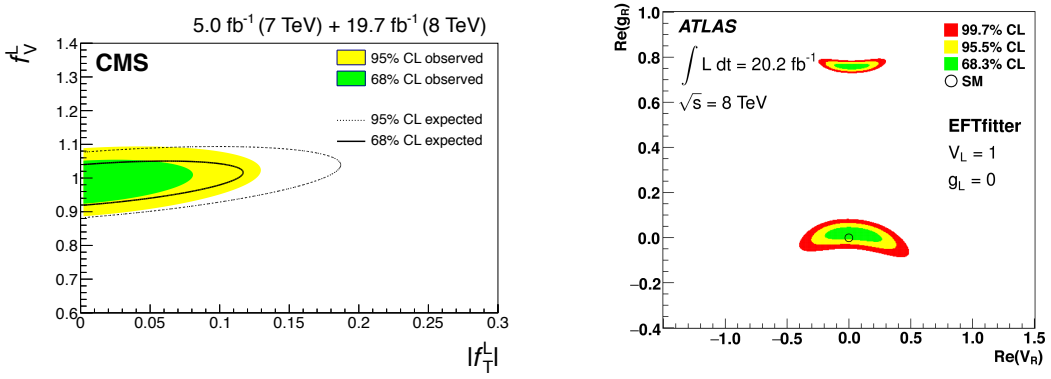

(a) (b)

Figure 4 – (a) Limits on the anomalous couplings V_{L} (labelled as $f_{\mathrm{V}}^{\mathrm{L}}$) and g_{L} (labelled as $f_{\mathrm{T}}^{\mathrm{L}}$) set by the CMS search using single-top events. (b) Limits on the anomalous couplings g_{R} and V_{R} set by the ATLAS measurement of the W-boson polarisation fractions.

The single top polarisation measurement is mainly sensitive to the imaginary part of g_{R}. The ATLAS measurements of the angular asymmetries for θ_l and θ_l^N are used in conjunction with analytical expressions [9,11,12] to extract limits on Im g_{R}. The correlation between the two asymmetry measurements (-0.05) is accounted for in the limit setting procedure. The limits set at the 95% confidence level are $\mathrm{Im}\, g_{\mathrm{R}} \in [-0.18,\, 0.06]$. The CMS experiment has designed a dedicated analysis to search for anomalous couplings in single-top events [13], where multivariate classifiers are used to separate the SM single-top events from potential contributions from non-zero anomalous couplings. No significant excess is seen and limits are set on different combinations of couplings. Figure 4 shows the limits set in the V_{L} and g_{L} plane.

The measurement of the W boson polarisation fractions by ATLAS has been used to set limits on the real parts of the anomalous couplings using the EFTfitter tool [14]. Figure 4 shows the limits set on the g_{R} and V_{R} couplings, under the assumptions $V_{\mathrm{L}} = 1$ and $g_{\mathrm{L}} = 0$. The different precision measurements sensitive to the Wtb vertex are complementary. In the interpretations done by the collaborations to date, it has always been necessary to set at least one of the couplings to the SM values. This motivates future combinations of these precision measurements, in order to obtain constraints that are free of SM assumptions and to exploit the complementary sensitivity of the different measurements.

3 Production of top quarks in association with vector bosons

The large integrated luminosity delivered by the LHC allows the possibility to study the rare production of top-quark pairs in association with either a Z or W boson ($t\bar{t}+V$). The production of $t\bar{t}+Z$ is particularly interesting, since it probes the top-Z coupling. ATLAS and CMS have both measured the $t\bar{t}+Z$ and $t\bar{t}+W$ cross-sections using the 13 TeV data [15,16]. The ATLAS measurement uses the 2015 dataset (corrsponding to a luminosity of 3.2 fb^{-1}), while the CMS measurement uses the data collected during the first half of 2016, which corresponds to an integrated luminosity of 12.9 fb^{-1}. The measurements are limited by statistics and hence this report will focus on the more precise CMS measurement.

The $t\bar{t}+V$ processes can produce final states with multiple-leptons and jets originating from b-quarks. Both experiments select events with either two leptons (electrons or muons) with the same-sign charge, three leptons or four leptons. For the dilepton channel, CMS selects events with at least 2 jets, at least one of which is identified as being likely to have originated from a b-quark (referred to as a b-jet) and then uses a multivariate technique to separate the signal from the $t\bar{t}$ background. To maximise the signal significance, the dilepton events are further categorised according to the dilepton charge and the number of jets and b-jets. The trilepton events are required to have at least 2 jets and events where a same-flavour opposite-sign charge (SFOS) lepton pair has an invariant mass close to the Z boson mass are rejected. The events are then categorised according to the number of jets and b-jets into twelve disjoint signal regions. The tetralepton events are required to have one SFOS lepton pair consistent with a Z boson and to contain at least two jets. In the $\mu\mu\mu\mu$, $eeee$ and $\mu\mu ee$ channels, events where the second SFOS lepton pair is consistent with a Z boson are rejected to reduce the background from ZZ events. Events are categorised according to whether or not they contain at least one b-jet.

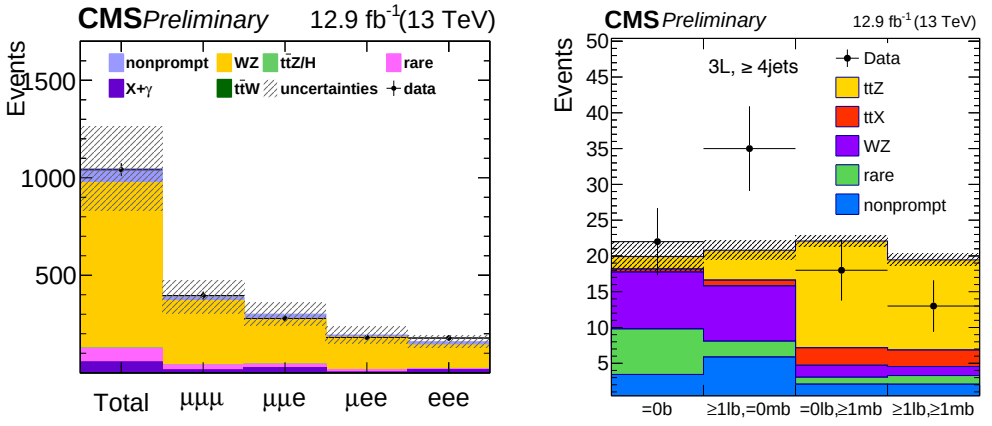

(a) (b)

Figure 5 – (a) Number of events in each lepton flavour channel for the WZ control region in the CMS $t\bar{t}+V$ measurement. (b) Number of events in the different b-jet categories in the CMS trilepton $t\bar{t}+V$ signal region with at least four jets, where mb refers to the number of jets passing a b-tagging requirement with an efficiency of 70% and lb refers to the number of jets failing the medium requirement and passing a loose requirement (with an efficiency of 85%). In both cases the data points in black are compared to the sum of the expected SM processes.

The background predictions use data-based methods for the the backgrounds where at least one lepton originates from non-prompt sources (leptons from heavy-flavour hadron decay, misidentified hadrons, muons from light-meson decay in flight, or electrons from unidentified photon conversions), while other background sources are estimated using simulation. The modelling of the backgrounds is checked in control regions. Figure 5 shows the number of events in each lepton flavour channel for a control region that selects events with three leptons and at most one jet. This region is dominated by WZ events and good agreement is seen between the

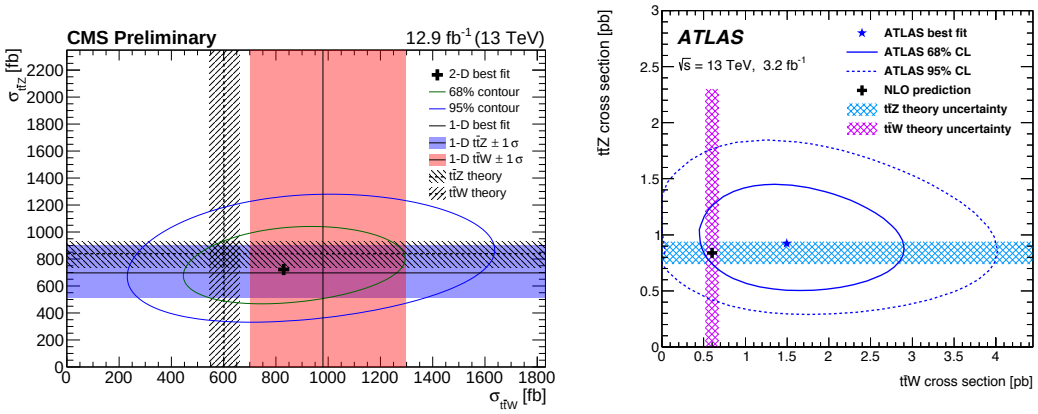

(a) (b)

Figure 6 – The measured cross-sections for the $t\bar{t}+W$ and $t\bar{t}+Z$ cross-sections are compared to the theoretical predictions for (a) the CMS results and (b) the ATLAS results.

data and the background prediction.

The $t\bar{t}$+W and $t\bar{t}$+Z cross-sections are extracted by making a combined fit to all the different signal regions. The data observed in the trilepton signal region with at least four jets are shown in Figure 5, where good agreement is seen between the data and the SM prediction. The measured cross-sections are shown in Figure 6 for both the ATLAS and CMS analyses. Agreement is seen between the data and the SM predictions. The measurements are dominated by the statistical uncertainty and hence measurements utilising larger datasets are eagerly awaited.

4 The top quark mass

The top quark mass is a fundamental parameter in the SM and precisely measuring its value is vital for establishing the consistency of the SM[17]. ATLAS has recently performed a measurement using top-quark pair events in the dilepton channel[18]. The events are selected from the 2012 data taken at $\sqrt{s} = 8$ TeV and the dataset corresponds to an integrated luminosity of 20.2 fb^{-1}. The selection requires exactly two leptons (either electrons or muons) and at least two jets, where at least one of the jets is required to be a b-jet. Additional requirements on the missing transverse momentum, the invariant mass of the lepton pair and the scalar sum of the p_T of the selected jets and leptons are applied to reduce the background from Z+jets events. The dilepton channel has the drawback that the prescence of two neutrinos makes the full reconstruction of the $t\bar{t}$ system challenging. The two jets with the highest probability to originate from b-quarks are taken as originating from the two top quarks. There are then two possible assignments of the leptons and b-jets. The combination that leads to the lowest average invariant mass of the two lepton-b-jet pairs ($m_{\ell b}$) is selected. The top mass can then be extracted from the $m_{\ell b}$ distribution. A phase-space restriction on the average p_T of the two lepton-b-jet pairs ($p_{\mathrm{T},\ell b}$) is used to obtain the smallest total uncertainty in m_{top}. The selected requirement is $p_{\mathrm{T},\ell b} > 120$ GeV and effectively selects a region where the systematic uncertainties are reduced.

The top-quark mass is extracted by performing a template fit to the $m_{\ell b}$ distribution. The signal templates are constructed by fitting Monte Carlo samples generated with different top quark masses with the sum of a Landau function and a Gaussian distribution. Figure 7 shows the templates for three different m_{top} values, demonstrating the sensitivity of the $m_{\ell b}$ distribution to the top-quark mass. The figure also shows the data compared to the template with the best fit value of the top-quark mass and good agreement is seen between the data and the fitted template. The top-quark mass is measured to be $m_{\mathrm{top}} = 172.99 \pm 0.41 \pm 0.74$ GeV, where the first uncertainty is the statistical uncertainty and the second is the total systematic uncertainty. The

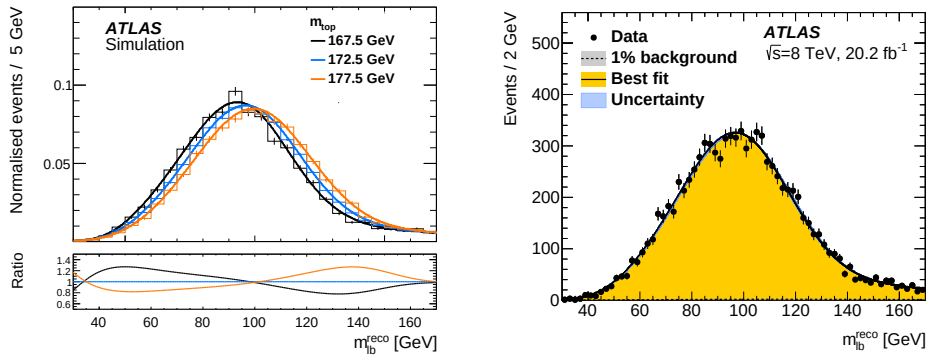

(a) (b)

Figure 7 – (a) Distribution of the $m_{\ell b}$ variable for templates and MC samples with different m_{top} values. (b) The template with the best fit for m_{top} is compared with the data (black points).

systematic uncertainty is dominated by the understanding of the jet energy scale (0.54 GeV), the MC modelling of top-quark pair events (0.35 GeV) and the jet energy scale for jets originating from b-quarks (0.30 GeV). The measurement is the most precise measurement of the top-quark mass in dilepton events to date.

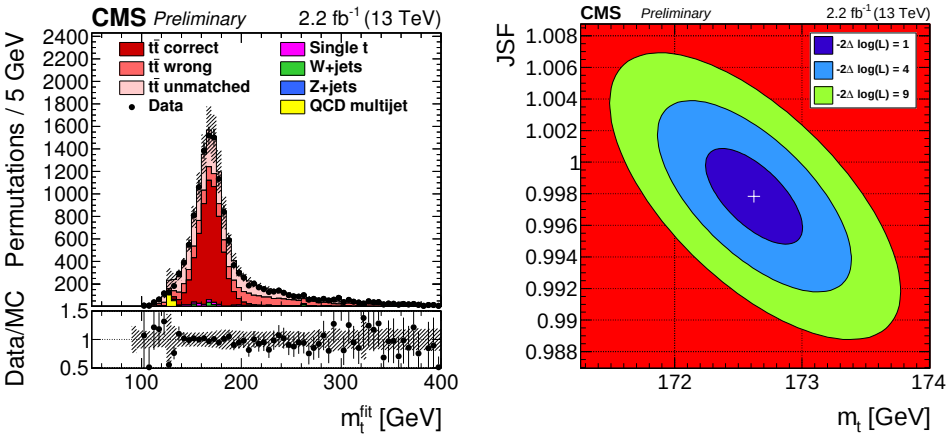

(a) (b)

Figure 8 – (a) Distribution of the reconstructed top-quark mass is compared to the simulation. (b) Fitted values for the top-quark mass and the JSF; the coloured contours show the statistical uncertainty.

The CMS collaboration has recently made the first measurement of the top-quark mass using the 13 TeV LHC data [19]. The analysis uses events with one muon and at least four jets (of which two must be b-jets) and the strategy closely follows the lepton+jets analysis that used the run 1 data [20]. A kinematic fit is applied to the selected events, where the fit constrains the W boson mass to 80.4 GeV [21] and the top and anti-top masses to be the same. The goodness-of-fit probability (gof) of the kinematic fit is required to be at least 0.2 in order to remove poorly reconstructed events. The top mass reconstructed from the kinematic fit (m_{top}^{fit}) is used along with the reconstructed W boson mass in a likelihood-fit to simultaneously extract the top-quark mass and the jet energy scale factor (JSF). The JSF allows the overall energy scale of jets to be constrained using the reconstructed W boson mass. In the likelihood-fit, events are weighted by their gof in order to reduce the impact of poorly reconstructed events. The reconstructed top mass distribution is shown in Figure 8, which shows the excellent mass resolution and good agreement between the data and the simulation. The top quark mass is measured to be $m_{\mathrm{top}} = 172.62 \pm 0.38 \pm 0.7$ GeV, where the first uncertainty is statistical and

the second is the total systematic uncertainty. The fitted JSF is in agreement with 1, as shown in Figure 8. The largest systematic uncertainties are from the jet energy scale (0.51 GeV) and the MC modelling of top-quark events (0.4 GeV). While the total uncertainty does not reach the precision achieved in run 1 [20], the understanding of the 13 TeV data is still at an early stage compared to run 1 and improvements in the uncertainties in the future can be anticipated.

5 Summary

The heavy mass of the top quark provides the opportunity to make precision measurements of a 'bare' quark. Recent measurements of W boson polarisation fractions in top-quark pair events and of top-quark polarisation in single-top quark events have probed the structure of the Wtb vertex. The measurements are all in agreement with the SM, with no signs of new physics. The high energy and large datasets provided by the LHC allow to measure the rare $t\bar{t}+Z$ and $t\bar{t}+W$ processes. The recent CMS measurement with 13 TeV data shows evidence for both processes and the larger datasets expected in the years ahead will allow for precision tests of the top-Z coupling. The top-quark mass has been measured to high precision with the LHC data. The recent dilepton measurement from ATLAS utilises a kinematic phase space selection to reduce the systematic uncertainties and CMS has made the first run 2 top mass measurement. Future prospects include a combination of the LHC run 1 results and precise measurements with the run 2 data.

References

1. ATLAS Collaboration, JINST 3 S08003 (2008).
2. CMS Collaboration, JINST 3 S08004 (2008).
3. ATLAS Collaboration, Eur. Phys. J. C **77** (2017) 264, arXiv:1612.02577 [hep-ex].
4. CMS Collaboration, Phys. Lett. B **762** (2016) 512, arXiv:1605.09047 [hep-ex].
5. G. Mahlon and S. Parke, Phys. Lett. B **476** (2000) 323, arXiv:hep-ph/9912458].
6. R. Schwienhorst, Q.-H. Cao, C.-P. Yuan and C. Mueller, Phys. Rev. D 83 (2011) 034019, arXiv:1012.5132 [hep-ph].
7. A. Brandenburg, Z. G. Si and P. Uwer, Phys. Lett. B **539** (2002) 235, arXiv:hep-ph/0205023].
8. ATLAS Collaboration, JHEP **1704**, 124 (2017), arXiv:1702.08309 [hep-ex].
9. J. A. Aguilar-Saavedra and J. Bernabu, Phys. Rev. D **93** (2016) 011301, arXiv:1508.04592 [hep-ph].
10. CMS Collaboration, JHEP **1604** (2016) 073, arXiv:1511.02138 [hep-ex].
11. J. A. Aguilar-Saavedra and J. Bernabu, Nucl. Phys. B **840** (2010) 349, arXiv:1005.5382 [hep-ph].
12. J. A. Aguilar-Saavedra and S. Amor dos Santos, Phys. Rev. D **89** (2014) 114009, arXiv:1404.1585 [hep-ph].
13. CMS Collaboration, JHEP **1702** (2017) 028, arXiv:1610.03545 [hep-ex].
14. N. Castro *et al.*, Eur. Phys. J. C **76** (2016) 432, arXiv:1605.05585 [hep-ex].
15. ATLAS Collaboration, Eur. Phys. J. C **77** (2017) 40, arXiv:1609.01599 [hep-ex].
16. CMS Collaboration, CMS-PAS-TOP-16-017 (2016), https://cds.cern.ch/record/2205283.
17. M. Baak *et al.* [Gfitter Group], Eur. Phys. J. C **74** (2014) 3046, arXiv:1407.3792 [hep-ph].
18. ATLAS Collaboration, Phys. Lett. B **761** (2016) 350, arXiv:1606.02179 [hep-ex].
19. CMS Collaboration, CMS-PAS-TOP-16-022 (2017), https://cds.cern.ch/record/2255834.
20. CMS Collaboration, Phys. Rev. D **93** (2016) 072004, arXiv:1509.04044 [hep-ex].
21. K. A. Olive, Chin. Phys. C 40 (2016) 100001.